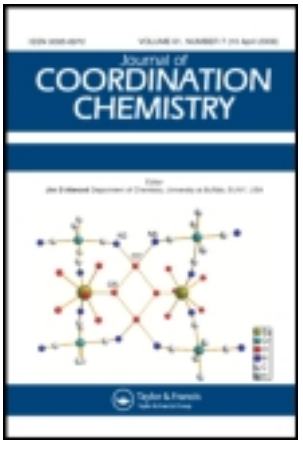

Journal of Coordination Chemistry
Publication details, including instructions for authors and subscription information:
http://www.tandfonline.com/loi/gcoo20

Synthesis, structure, DNA binding, and cleavage activity of two copper(II) complexes

Chunyan Gao [a], Xiaofang Ma [a b], Jing Lu [a], Zhigang Wang [a], Jinlei Tian [a] & Shiping Yan [a]

[a] Department of Chemistry, Nankai University, Tianjin 300071, China

[b] Basic Medical College, Zhengzhou University, Zhengzhou 450001, China

Published online: 20 Jun 2011.

To cite this article: Chunyan Gao, Xiaofang Ma, Jing Lu, Zhigang Wang, Jinlei Tian & Shiping Yan (2011) Synthesis, structure, DNA binding, and cleavage activity of two copper(II) complexes, Journal of Coordination Chemistry, 64:12, 2157-2169, DOI: 10.1080/00958972.2011.587514

To link to this article: http://dx.doi.org/10.1080/00958972.2011.587514

Journal of Coordination Chemistry
Vol. 64, No. 12, 20 June 2011, 2157–2169

Synthesis, structure, DNA binding, and cleavage activity of two copper(II) complexes

CHUNYAN GAO†, XIAOFANG MA†‡, JING LU†, ZHIGANG WANG†, JINLEI TIAN† and SHIPING YAN*†

†Department of Chemistry, Nankai University, Tianjin 300071, China
‡Basic Medical College, Zhengzhou University, Zhengzhou 450001, China

(*Received 20 January 2011; in final form 12 April 2011*)

Two copper(II) complexes, $[Cu_2(L^1)_2(H_2O)]_\infty$ (**1**) and $\{[Cu_2(L^2)_2(H_2O)]\cdot H_2O\}_\infty$ (**2**), have been synthesized and characterized by elemental analysis, UV-visible absorption spectra, and single-crystal X-ray diffraction. H_2L^1 is an amino acid Schiff base derived from condensation of N-(2-hydroxybenzaldehyde) and L-methionine. H_2L^2 is a reduced product of H_2L^1 by sodium borohydride (scheme 1). Both complexes consist of one-dimensional covalently bonded polymeric chains. Complex **1** has two crystallographic independent copper centers. Cu1 has a distorted octahedral geometry and Cu2 a square pyramid. The copper(II)'s are bridged by carboxylate with a Cu1–Cu2 separation of 3.6399(5) Å. Complex **2** is a double phenolate-bridged complex with a Cu1–Cu2 separation of 3.0148(7) Å, where each copper is square pyramidal. Binding of the complexes with Calf thymus DNA (CT-DNA) has been investigated by UV-visible spectra and fluorescence quenching, showing intercalation to CT-DNA. DNA cleavage experiments have been also investigated by agarose gel electrophoresis. Both complexes show oxidative DNA cleavage in the presence of H_2O_2/sodium ascorbate. The reactive oxygen species responsible for the DNA cleavage is likely singlet oxygen ($^1O_2$).

Keywords: Copper(II) complexes; Crystal structures; Reduced Schiff-base ligand; DNA cleavage; Reactive oxygen species

1. Introduction

Interactions of metal complexes with DNA have been the subject of intense investigation for new reagents for biotechnology and medicine. Transition metal complexes which provide routes toward rational drug design and chemical probes for DNA are well studied for application as artificial nucleases. Because of their diverse structural features and the possibility to tune redox potentials through choice of ligands [1–6], a number of metal complexes have been used as probes for DNA structure in solution, as agents for mediation of strand scission of duplex DNA, and as chemotherapeutic agents [7–10]. Transition metal complexes containing Schiff-base ligands and their reduced products are often used as artificial chemical nucleases and some complexes have proved to be efficient DNA cleavage reagents. Most Schiff-base complexes are capable of promoting the cleavage of plasmid DNA in

*Corresponding author. Email: yansp@nankai.edu.cn

ISSN 0095-8972 print/ISSN 1029-0389 online
DOI: 10.1080/00958972.2011.587514

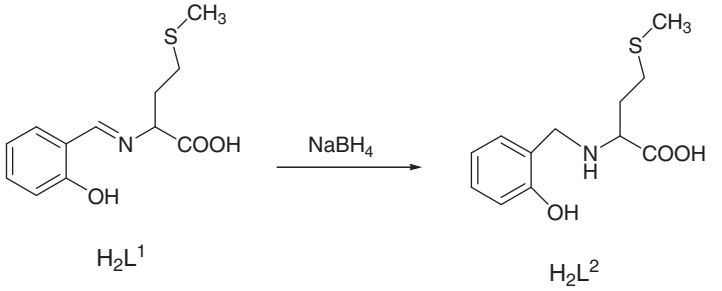

H_2L^1 H_2L^2

Scheme 1. Schematic structures of H_2L^1 and H_2L^2.

a pH-dependent reaction, even in the absence of molecular dioxygen, probably through a hydrolytic mechanism [11, 12]. Most studies of metal complexes of Schiff-base ligands containing salicylaldehyde and amino acids have focused on the binding mode of these ligands [13–20]. Structural studies on metal complexes of reduced Schiff-base ligands, derived from various amino acids and salicylaldehyde, are well documented [21–31]. Systematic investigations on the DNA binding and cleavage activities of Schiff-base complexes and their reduced products may provide important information for design of new chemical nucleases.

In this article, we selected two biologically relevant amino acid Schiff bases H_2L^1 and their reduced product H_2L^2 as ligands [32, 33] (scheme 1) and obtained two new copper(II) complexes. The Schiff bases and their reduced products from amino acid and salicylaldehyde are chiral and multidentate, showing versatility by forming molecules with different nuclearities as well as H-bonded networks in the presence of metals. The copper(II)'s of **1** are bridged by carboxylate oxygen while **2** is phenolate bridged. Vittal and co-workers have structurally characterized a number of Cu(II) complexes of related ligands with alanine, valine, glycine, tryptophan, and tyrosine; all their reported complexes have a phenolate-bridged binuclear structure [34]. All Cu(II) complexes of reduced Schiff bases of amino acid–salicylaldehyde ligands isolated from alcohol or water, irrespective of amino acid used, are phenolate-bridged binuclear complexes [35]. Interactions between calf thymus DNA (CT-DNA) and the complexes were investigated by UV absorption and fluorescence spectroscopy. DNA cleavage experiments in the presence of hydrogen peroxide/sodium ascorbate are also determined. Histidine inhibits the oxidative cleavage, suggesting that singlet oxygen ($^1O_2$) is involved in the DNA degradation.

2. Experimental

2.1. *Materials and methods*

All reagents and chemicals were purchased from commercial sources and used as received. Elemental analyses (C, H, and N) were obtained on a *Perkin Elmer* analyzer model 240. Infrared spectra were recorded as KBr pellets using a *Perkin Elmer* FT–IR spectrometer from 4000 to 400 cm^{-1}. Electronic spectra were measured on a *JASCO*

V-570 spectrophotometer. Fluorescence spectral data were obtained on a *MPF-4* fluorescence spectrophotometer at room temperature. CT-DNA, pBR322 DNA, agarose (molecular biology grade), and ethidium bromide (EB) were all purchased from the Sino-American Biotechnology Company. The Tris–HCl buffer solution was prepared using deionized, sonicated triple-distilled water. Gel electrophoresis experiments were performed by incubation at 37°C for 3 h as follows: pBR322 DNA (33 μmol L^{-1}), Cu(II) complexes, and H_2O_2/sodium ascorbate in 50 m mol L^{-1} Tris–HCl/18 m mol L^{-1} NaCl buffer (pH 7.2). The samples were electrophoresed for 3 h at 70 V on 1% agarose gel using Tris–boric acid–EDTA buffer, pH 7.2. After electrophoresis, the gel was stained using 1 mg mL^{-1} EB and analyzed using a UVITEC automatic gel-imaging system.

2.2. *Preparation of compounds*

2.2.1. Synthesis of H_2L^1 and H_2L^2. H_2L^1 is an amino acid Schiff base derived from condensation of L-methionine and 2-hydroxybenzaldehyde according to the literature method [36]; H_2L^2 is a reduced product of H_2L^1 by sodium borohydride. Anal. Found (%): C, 56.95; H, 5.99; and N, 5.47. Calcd (%) for $C_{12}H_{15}NO_3S$ (**1**): C, 56.90; H, 5.97; and N, 5.53. For **2**, Anal. Found (%): C, 56.53; H, 6.79; and N, 5.42. Calcd (%) for $C_{12}H_{17}NO_3S$ (**2**): C, 56.45; H, 6.71; and N, 5.49. FT–IR (KBr, cm^{-1}) for **1**: 3450, ν(OH); 1680, ν(C=N); 1604, ν_{as}(COO); 1408, ν_s(COO); for **2**: 3445, ν(OH); 3118, ν(N–H); 1634, ν(C–N); 1605, ν_{as}(COO); and 1410, ν_s(COO).

2.2.2. Synthesis of $[Cu_2(L^1)_2(H_2O)]_\infty$ (1). A solution of H_2L^1 (0.2 mmol) and 0.4 mmol LiOH in EtOH : H_2O (1 : 1 v/v, 10 mL) was added dropwise to a solution of 0.2 mmol $CuCl_2 \cdot 6H_2O$ in EtOH : H_2O (1 : 1 v/v, 10 mL). After stirring for 24 h, the solution was filtered and the filtrate left in air at room temperature. After 4 weeks, green crystals suitable for X-ray diffraction were obtained. The crystals were collected by filtration, washed with Et_2O, and dried over silica gel (yield 43%). Anal. Found (%): C, 44.78; H, 4.43; and N, 4.12. Calcd (%) for $C_{24}H_{28}Cu_2N_2O_7S_2$: C, 44.51; H, 4.36; and N, 4.33. FT–IR bands (KBr phase): 1598 cm^{-1}, ν_{as}(COO); 1409 cm^{-1}, ν_s(COO); 3019 cm^{-1}, ν(N–H); 3424 cm^{-1}, ν_s(H_2O and/or OH).

2.2.3. Synthesis of $\{[Cu_2(L^2)_2(H_2O)] \cdot H_2O\}_\infty$ (2). Complex **2** was prepared by similar procedures to **1** using $CuAc_2 \cdot H_2O$ instead of $CuCl_2 \cdot 6H_2O$. Yield: 46%. Anal. Found (%): C, 43.60; H, 4.95; and N, 4.02. Calcd (%) for $C_{24}H_{34}Cu_2N_2O_8S_2$: C, 43.17; H, 4.83; and N, 4.20. FT–IR bands (KBr phase): 1613 cm^{-1}, ν_{as}(COO); 1418 cm^{-1}, ν_s(COO); 2924 cm^{-1}, ν_s(N–H); 3421 cm^{-1}, and ν_s(H_2O and/or OH).

2.3. *X-ray crystallography*

Diffraction measurements for **1** and **2** were made on a Bruker Smart 1000 CCD area detector equipped with graphite-monochromated Mo-Kα radiation ($\lambda = 0.71070$ Å) using the ω-scan technique. Lorentz polarization and absorption correlations were applied using the multiscan program [37]. The structures were solved by direct methods

Table 1. Crystallographic data for **1** and **2**.

Complex	**1**	**2**
Empirical formula	$C_{24}H_{28}Cu_2N_2O_7S_2$	$C_{24}H_{34}Cu_2N_2O_8S_2$
Formula weight	647.68	669.73
Temperature (K)	113(2)	294(2)
Wavelength (Å)	0.71070	0.71070
Crystal system	Orthorhombic	Orthorhombic
Space group	$P2_12_12_1$	$P2_12_12_1$
Unit cell dimensions (Å)		
a	5.0365(2)	10.3143(17)
b	13.2159(6)	10.4469(17)
c	37.354(2)	25.949(4)
Volume (Å^3), Z	2486.4(2), 4	2796.1(8), 4
Calculated density (g cm^{-3})	1.73	1.591
$F(000)$	1328	1384
θ range for data collection (°)	2.18–25.01	2.10–25.02
Limiting indices	$-5 \le h \le 5$, $-15 \le k \le 15$, $-44 \le l \le 39$	$-12 \le h \le 11$, $-12 \le k \le 12$, $-18 \le l \le 30$
Reflections collected	18,218	14,569
Independent reflections	4347 [R(int) = 0.0485]	4950 [R(int) = 0.0368]
Goodness-of-fit on F^2	1.076	1.066
Final R indices [$I > 2\sigma(I)$]	$R_1 = 0.0274$, $wR_2 = 0.0588$	$R_1 = 0.0303$, $wR_2 = 0.0633$
R indices (all data)	$R_1 = 0.0295$, $wR_2 = 0.0599$	$R_1 = 0.0382$, $wR_2 = 0.0662$
Largest difference peak and hole (e Å^{-3})	0.282 and −0.403	0.379 and −0.284

and refined with full-matrix least-squares technique using SHELXS-97 and SHELXL-97 [38]. Anisotropic thermal parameters were assigned to all non-hydrogen atoms. Hydrogens attached to carbons were generated geometrically and allowed to ride along with the atoms to which they were attached. Analytical expressions of neutral atom scattering factors were employed and anomalous dispersions incorporated. A summary of the crystal data is given in table 1 and selected bond angles and distances are listed in table 2.

2.4. *DNA-binding and cleavage experiments*

All studies on the interaction of the complexes with CT-DNA were carried out at room temperature in triple-distilled water buffer containing 5 m mol L^{-1} Tris–HCl/50 mM NaCl and adjusted to pH 7.2 with hydrochloric acid. Relative binding of the complexes to CT-DNA was studied by UV-visible absorption and fluorescence spectroscopy. Solutions of CT-DNA gave a ratio of UV absorbance at 260 and 280 nm, A_{260}/A_{280}, of 1.8–1.9, indicating that the DNA was sufficiently free of protein [39]. The stock solution of CT-DNA was prepared in Tris–HCL/NaCL buffer, pH = 7.2 (stored at 4°C and used within 4 days). The concentration of CT-DNA was determined by absorption spectroscopy using the known molar extinction coefficient of 6600 (mol L^{-1})$^{-1}$ cm^{-1} at 260 nm [40]. UV absorption spectroscopy experiments were conducted by adding CT-DNA solution to solutions of complexes (1.5×10^{-4} mol L^{-1}) at different concentrations. The binding constant, K_b, was determined using the following equation [41]:

$$[\mathrm{DNA}]/(\varepsilon_A - \varepsilon_F) = [\mathrm{DNA}]/(\varepsilon_B - \varepsilon_F) + 1/K_b(\varepsilon_B - \varepsilon_F) \quad (1)$$

Table 2. Selected bond distances (Å) and angles (°) for **1** and **2**.

Complex **1**		Complex **2**	
Cu(1)–O(4)	1.910(2)	Cu(1)–O(3)	1.928(2)
Cu(1)–N(2)	1.942(2)	Cu(1)–O(6)	1.938(2)
Cu(1)–O(5)	2.011(2)	Cu(1)–O(4)	1.962(2)
Cu(1)–O(2)	2.0672(19)	Cu(1)–N(2)	1.973(3)
Cu(1)–O(7)	2.357(2)	Cu(1)–O(2)A	2.4691(3)
Cu(1)–O(6)A	2.6566(1)	Cu(2)–O(1)	1.924(2)
Cu(2)–O(1)	1.887(2)	Cu(2)–O(3)	1.942(2)
Cu(2)–N(1)	1.909(2)	Cu(2)–O(4)	1.983(2)
Cu(2)–O(5)#1	1.9644(18)	Cu(2)–N(1)	1.999(3)
Cu(2)–O(2)	2.053(2)	Cu(2)–O(5)	2.210(2)
Cu(2)–O(3)A	2.5080(1)		
O(4)–Cu(1)–N(2)	93.08(9)	O(3)–Cu(1)–O(6)	100.01(10)
O(4)–Cu(1)–O(5)	172.83(8)	O(3)–Cu(1)–O(4)	79.24(9)
N(2)–Cu(1)–O(5)	81.44(9)	O(6)–Cu(1)–O(4)	168.15(11)
O(4)–Cu(1)–O(2)	93.79(8)	O(3)–Cu(1)–N(2)	168.19(11)
N(2)–Cu(1)–O(2)	162.73(9)	O(6)–Cu(1)–N(2)	83.47(11)
O(5)–Cu(1)–O(2)	92.76(7)	O(4)–Cu(1)–N(2)	95.02(10)
O(4)–Cu(1)–O(7)	92.82(8)	O(3)–Cu(1)–Cu(2)	38.99(7)
N(2)–Cu(1)–O(7)	100.82(9)	O(6)–Cu(1)–Cu(2)	138.56(7)
O(5)–Cu(1)–O(7)	83.73(8)	O(4)–Cu(1)–Cu(2)	40.44(6)
O(2)–Cu(1)–O(7)	94.64(8)	N(2)–Cu(1)–Cu(2)	135.18(8)
O(5)–Cu(2)–O(2)#1	96.26(8)	O(1)–Cu(2)–O(3)	168.33(11)
O(1)#1–Cu(2)–N(1)#1	93.71(9)	O(1)–Cu(2)–O(4)	98.50(9)
O(1)#1–Cu(2)–O(5)	87.63(8)	O(3)–Cu(2)–O(4)	78.42(9)
N(1)#1–Cu(2)–O(5)	174.33(9)	O(1)–Cu(2)–N(1)	85.20(11)
O(1)#1–Cu(2)–O(2)#1	171.07(8)	O(3)–Cu(2)–N(1)	94.86(10)
N(1)#1–Cu(2)–O(2)#1	83.21(9)	O(4)–Cu(2)–N(1)	164.20(11)
Cu(2)#2–O(5)–Cu(1)	132.60(9)	O(1)–Cu(2)–O(5)	97.46(10)
O(2)–Cu(2)–O(3)A	97.572(1)	O(3)–Cu(2)–O(5)	94.18(10)
N(1)–Cu(2)–O(3)A	93.255(2)	O(4)–Cu(2)–O(5)	100.93(10)
O(1)–Cu(2)–O(3)A	90.953(2)	N(1)–Cu(2)–O(5)	93.76(12)
O(5)–Cu(2)–O(3)A	81.207(2)		

Symmetry transformations used to generate equivalent atoms: #1 $x-1, y, z$; #2 $x+1, y, z$ for **1**.

Here ε_A, ε_F, and ε_B correspond to A_{obsd}/[complex], the extinction coefficient for the free complex, and the extinction coefficient for the complex in the fully bound form, respectively.

By the fluorescence spectral method, the relative binding of the complexes to CT-DNA was studied with an EB-bound CT-DNA solution in 5 m mol L^{-1} Tris–HCl/NaCl buffer (pH = 7.2). Fluorescence intensities at 610 nm (510 nm excitation) were measured at different concentrations of complexes. The emission intensity showed reduction upon addition of the complex.

Oxidative cleavage of supercoiled (SC) pBR322 DNA by the complexes was studied by agarose gel electrophoresis. The reaction was carried out by mixing 4 μL SC DNA (0.1 μg μL^{-1}, 16.5 μ mol L^{-1}), 8 μL of the complex solution (120 μ mol L^{-1}), and 2 μL 50 m mol L^{-1} Tris–(hydroxymethylmethane–HCl) (Tris–HCl) buffer (pH = 7.2) containing 18 m mol L^{-1} NaCl with 1 μL H_2O_2/1 μL sodium ascorbate to yield a total volume of 16 μL. The sample was incubated at 37°C, followed by addition of loading buffer containing 0.25% bromophenol blue, and 50% glycerol, 0.61% Tris, and the solution was finally loaded on 1% agarose gel containing 1.0 μg mL^{-1} EB.

Electrophoresis was carried out for 3 h at 70 V in TBE buffer (45 m mol L^{-1} Tris, 45 m mol L^{-1} H_3BO_3, 1 m mol L^{-1} EDTA, pH 8.0). Bands were visualized by UV light and photographed. The extent of cleavage of the SC DNA was determined by measuring intensities of the bands using the Gel Documentation System [42, 43]. Mechanistic investigation of the cleavage of pBR322 DNA was carried out in the presence of standard radical scavengers and reaction inhibitors. These reactions were carried out by adding scavengers, dimethyl sulfoxide (DMSO), superoxide dismutase (SOD), ethylenediaminetetraacetic acid disodium salt (EDTA), or histidine to SC DNA. Cleavage was initiated by addition of complex and quenched with 2 μL of loading buffer. Further analysis was carried out by the above standard method.

3. Results and discussion

3.1. *Description of the crystal structures of 1 and 2*

Single-crystal X-ray analysis reveals that **1** and **2** crystallize in the orthorhombic space group $P2_12_12_1$ and they are both one-dimensional (1-D) coordination polymers with the binuclear copper fragments as building blocks. The labeling schemes of the binuclear unit of **1** and **2** are shown in figures 1 and 2, and segments of the 1-D chain for **1** and **2** are given in figures 3 and 4. The structure of **1** consists of $[Cu_2(\mathbf{L}^1)_2(H_2O)]$ building units generating a 1-D polymeric chain reinforced by a carboxylate–copper weak interaction. As shown in figure 1, each $[Cu_2(\mathbf{L}^1)_2(H_2O)]$ contains two discrete Cu's and two tridentate Schiff-base ligands. The two copper(II) atoms are bridged by the carboxylate with Cu1–Cu2 separation of 3.6399(5) Å. Two kinds of weak Cu–O interactions (Cu1–O6A, 2.659 Å; Cu2–O3A, 2.509 Å) exist among $[\mathbf{Cu_2(L^1)_2}(H_2O)]$ units. In **1**, Cu1

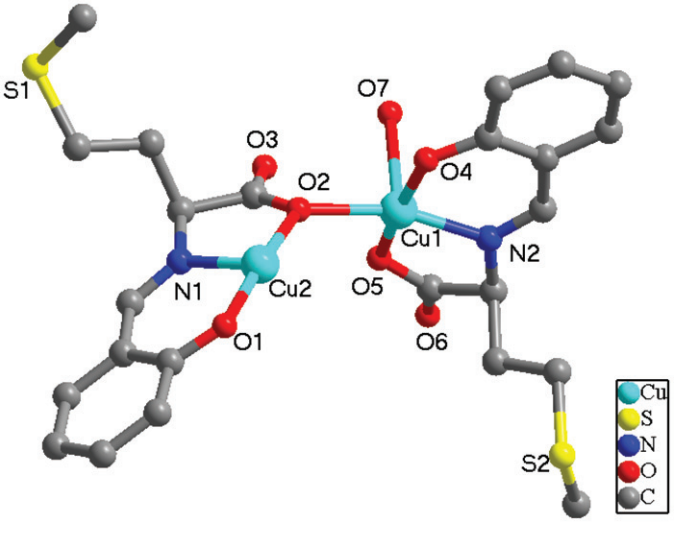

Figure 1. The labeling scheme of binuclear unit of **1**; hydrogens are omitted for clarity.

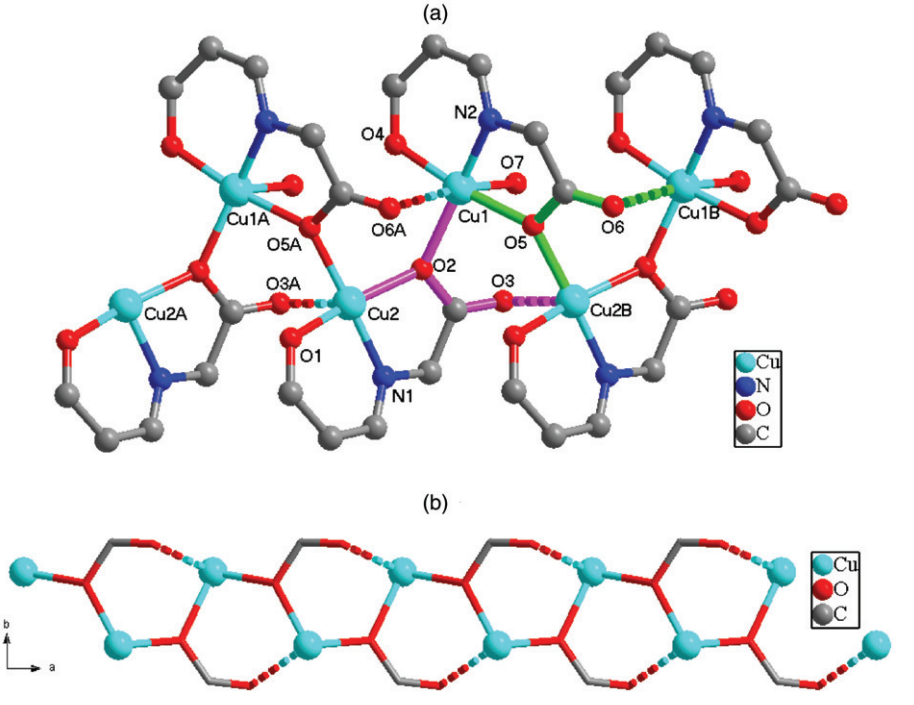

Figure 2. ((a) and (b)) Segment of the 1-D chain through weak Cu–O coordination for **1**; hydrogens, sulfurs and some carbons are omitted for clarity.

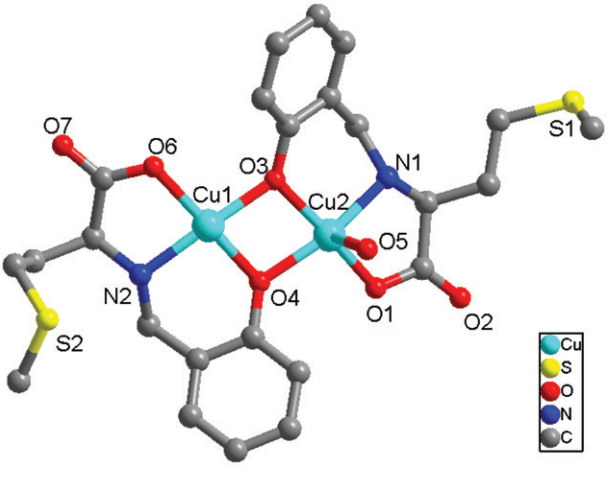

Figure 3. The labeling scheme of binuclear unit of **2**; hydrogens are omitted for clarity.

is six-coordinate with a O_5N donor set derived from one nitrogen, three carbonyl oxygens, one phenol oxygen of the ligand, and one coordinated water in a distorted octahedral geometry, while Cu2 has a square-pyramidal stereochemistry ($\tau = 0.038$) with a O_4N donor set.

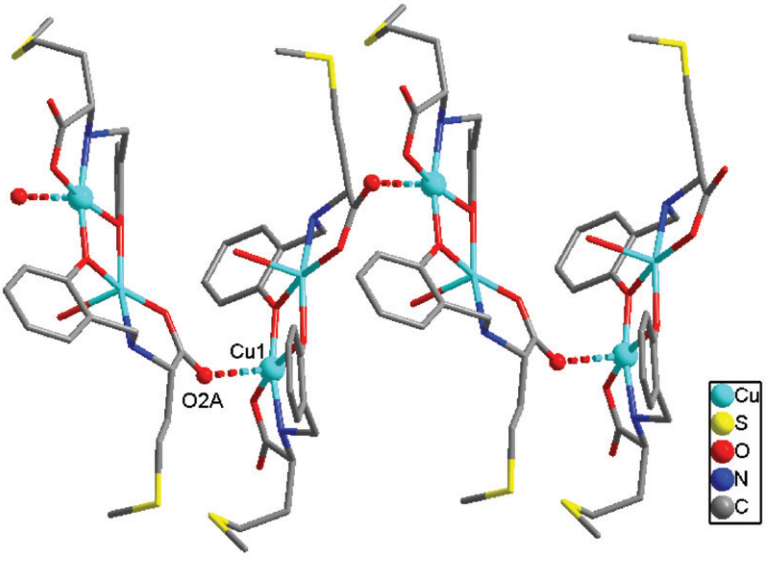

Figure 4. Segment of the 1-D chain through weak Cu–O interaction for **2**; hydrogens are omitted for clarity.

The structure of **2** consists of the basic bis-phenoxo-bridged binuclear building block $[Cu_2(\mathbf{L}^2)_2(H_2O)]$ (figure 2) in which both Cu's have approximate square-pyramidal geometry ($\tau = 0.008$ for Cu1 and 0.080 for Cu2) similar to analogues [22]. In **2**, two phenolato oxygen molecules, an imine nitrogen, and a carboxylate oxygen form the base of a square with normal Cu–O or Cu–N bond distances. The axial coordination of Cu1 is provided by carboxylate (O2A) from another binuclear unit with the axial Cu1–O2A distance of 2.469 Å, forming a helical polymeric chain as shown in figure 4. The axial site of Cu2 is occupied by a water (O5) with Cu2–O5 distance of 2.211 Å. Thus **2** contains two unique Cu centers with Cu1–Cu2 distance of 3.0148 Å. Unlike its Schiff base counterpart, the deprotonated dianionic ligand $(L^2)^{2-}$ has a more flexible backbone and each ligand coordinated to Cu in a *mer* fashion, as evident from O4–Cu1–O6 and O1–Cu2–O3 angles. In each $(L^2)^{2-}$, the chiral C-center has the absolute configuration S. After complexation with Cu, the nitrogen of $(L^2)^{2-}$ becomes chiral. In **2**, the absolute configuration of nitrogen is also S. Thus, the generation of the new chiral center is homogeneous with respect to the original chiral C-center. The same conformation preference at chiral carbon and amine N has been observed in complexes of other reduced Schiff-base ligands [35].

Hydrogen bonding networks exist in these complexes. For **2**, there are complicated intramolecular and intermolecular hydrogen bonds among carboxyl oxygen, phenolic oxygen and coordinated water. Only intramolecular hydrogen bonds exist in **1**.

3.2. *DNA binding studies*

DNA binding is critical for DNA cleavage in most cases. Therefore, the binding ability of the complexes to CT-DNA was studied using UV-Vis absorption and fluorescence spectroscopy.

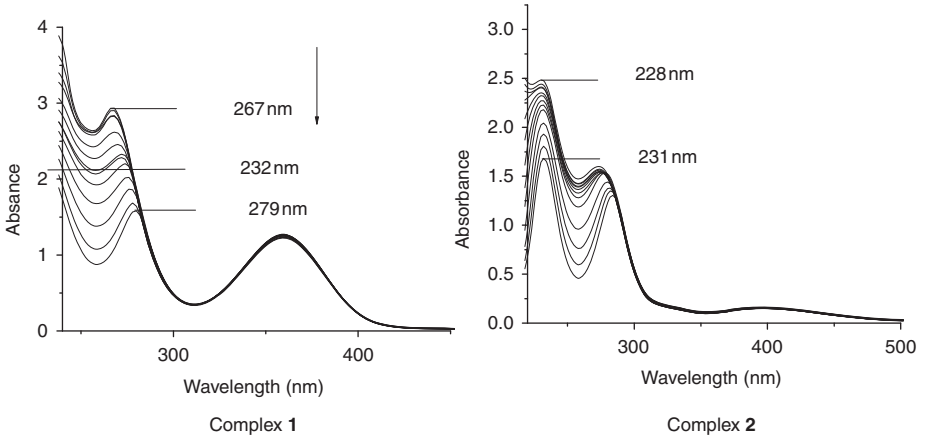

Figure 5. Electronic absorption spectra of **1** and **2** in the absence (dashed line) and presence (solid line) of increasing amounts of CT-DNA ($0 - 7.9 \times 10^{-4}$ mol L^{-1}) at room temperature in 5 m mol L^{-1} Tris–HCl/NaCl buffer (pH 7.2). The dashed lines indicate the free complexes.

3.2.1. UV-visible absorption spectroscopy. Electronic absorption spectroscopy is a useful technique for DNA-binding studies of metal complexes. Typical titration curves for complexes are shown in figure 5. Absorptions at 267 and 279 nm for **1**, and 228 and 231 nm for **2** are attributed to intraligand π–π^* transition. Upon addition of increasing amount of CT-DNA (0–7.9×10^{-4} mol L^{-1}) to the complexes (1.5×10^{-4} mol L^{-1}), 24.5–27.0% hypochromism and slight red shift (3–12 nm) were observed. The extent of hypochromism is consistent with the strength of intercalative interaction [44–46]. From the observed spectral changes, values of the intrinsic binding constants K_b (4.91×10^3 (mol L^{-1})$^{-1}$ for **1** and 8.75×10^3 (mol L^{-1})$^{-1}$ for **2**) were determined by regression analysis using equation (1). The K_b values are much smaller than those reported for typical classical intercalators (EB–DNA, 3.3×10^5 (mol L^{-1})$^{-1}$ in 50 mmol L^{-1} Tris–HCl/1.0 mol L^{-1} NaCl buffer, pH 7.5) [47]. The low binding constant and small red shift of the metal-to-ligand charge-transfer (MLCT) band suggest that **1** and **2** bind with DNA *via* partial intercalation.

3.2.2. Fluorescence spectroscopic studies. To further clarify the binding of these complexes, fluorescence spectral measurements were carried out on CT-DNA by varying the concentration of the complexes. The binding of the compounds to CT-DNA is evaluated by the fluorescence emission intensity of EB bound to DNA as a probe. EB shows reduced emission intensity in buffer because of quenching by solvent molecules and significant enhancement when bound to DNA. Binding of the complexes to DNA decreases the emission intensity and the extent of reduction of the emission intensity gives a measure of the DNA binding of the complexes and stacking interaction (intercalation) between the adjacent DNA base pairs [48]. The fluorescence quenching of EB bound to DNA by the two complexes is shown in figure 6 with fluorescence intensities at 610 nm (510 nm excitation) measured at different complex concentrations. The emission intensity is reduced on addition of the complex.

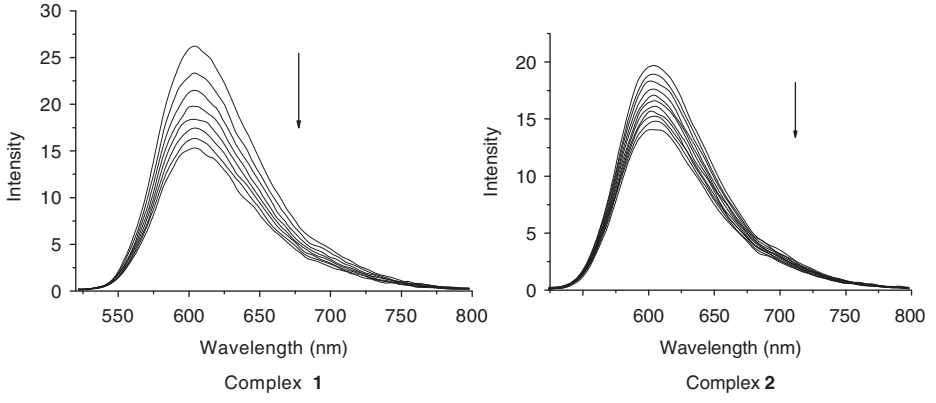

Figure 6. Fluorescence emission spectra for **1** and **2** ($\lambda_{ex} = 510$ nm) of the EB–DNA system (2.4×10^{-6} mol L^{-1} EB, 4.0×10^{-3} mol L^{-1} CT-DNA) in the absence and presence of 1.5×10^{-4} mol L^{-1} complex (40 μL per scan) and plot of I_0/I *vs.* [complex]. I_0 is the emission intensity of EB–DNA in the absence of complex and I the emission intensity of EB–DNA in the presence of complexes.

3.2.3. Nuclease activity of the complexes. Schiff-base complexes of copper [49] and their reduced products are often used as artificial chemical nucleases with some being efficient DNA cleavage reagents. The ability of the complexes to mediate DNA cleavage was assayed using agarose gel electrophoresis at physiological pH and temperature. When supercoiled circular pBR322 DNA is subjected to electrophoresis, relatively fast migration is observed for the intact supercoiled form (Form I). If scission occurs on one strand (nicking), the supercoiled form relaxes to generate a slower moving open nicked form (Form II), and if both strands are cleaved, a linear form (Form III) that migrates between Forms I and II will be observed.

The data of the gel electrophoretic separations of plasmid pBR322 DNA induced by **1** and **2** are presented in figures 7–9. Both complexes promote oxidative damage of DNA under physiological conditions (pH 7.2, 37°C) and the DNA cleavage activities of the complexes are concentration-dependent (see figure 7(a) and (b) for **1** and 7(c) for **2**). With increase of complex concentration, supercoiled DNA decreases and nicked circular DNA gradually increases. Figure 8(a) and (b) shows that in the presence of reductive reagents, such as H_2O_2, sodium ascorbate, and mercaptoethanol, the complexes display more effective DNA cleavage. In studies of reaction mechanism, we selected sodium ascorbate as reducing agent. In order to assess whether reactive oxygen species (ROS), such as singlet oxygen and/or hydroxyl radical, were involved in DNA cleavage, several radical scavengers were examined. As shown in figure 9(a) and (b), the experimental data indicate that hydroxyl radical can be ruled out in the DNA cleavage reactions, and singlet oxygen is therefore likely the reactive species.

4. Conclusions

Two new copper(II) complexes have been synthesized and structurally characterized, and the abilities of binding with CT-DNA and supercoiled plasmid DNA cleavage activities of the complexes have been studied. Complexes **1** and **2** bind to CT-DNA with

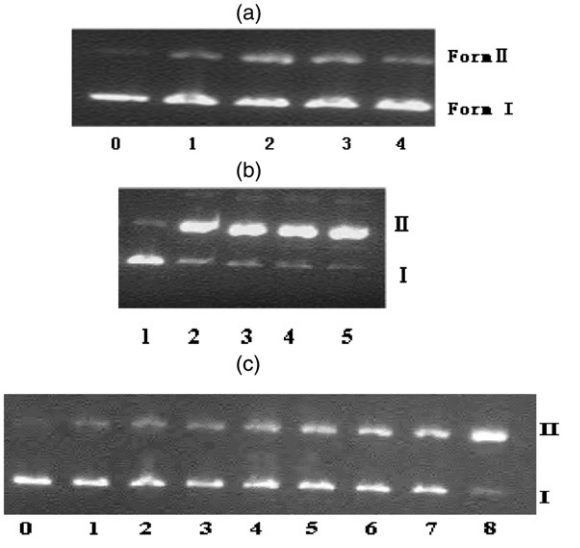

Figure 7. Gel electrophoresis diagrams showing the cleavage of pBR322 DNA (33 μmol L^{-1}) by **1** or **2** at different concentrations in Tris–HCl/NaCl buffer (pH = 7.2) and incubated 3 h, 37°C. (a) For **1**: Lane 0: DNA control; lanes 1–4, DNA + **1** (40 μmol L^{-1}; 80 μmol L^{-1}; 120 μmol L^{-1}; 160 μmol L^{-1}, respectively). (b) For **1**: lane 1, DNA + ascorbic acid (25 μmol L^{-1}); lanes 2–5, DNA + sodium ascorbate (25 μM) + **1** (20, 40, 60, 80 μmol L^{-1}, respectively). (c) For **2**: Lane 0, DNA control; lanes 1–8, DNA + **2** (11, 22, 33, 44, 55, 66, 77, 88 μmol L^{-1}).

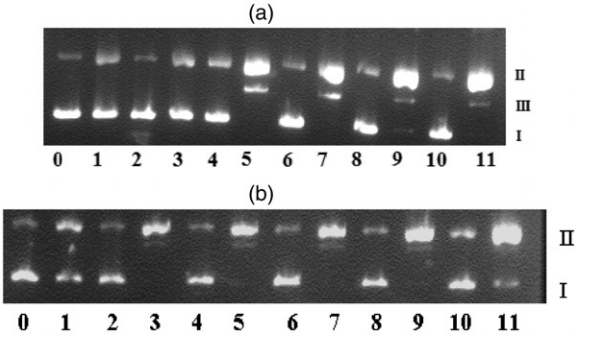

Figure 8. Agarose gel electrophoresis diagrams showing the cleavage of pBR322 DNA (33 μmol L^{-1}) by **1** or **2** treated with different reducing reagents in Tris–HCl/NaCl buffer (pH 7.2) and incubated 3 h, 37°C. Lane 0, DNA control. (a) For **1**: Lane 0, DNA control; lane 1, DNA + **1** (20 μmol L^{-1}); lane 2, DNA + H_2O_2 (25 μmol L^{-1}); lane 3, DNA + H_2O_2 (25 μmol L^{-1}) + **1** (40 μmol L^{-1}); lane 4, DNA + sodium ascorbate (25 μmol L^{-1}); lane 5, DNA + sodium ascorbate (25 μmol L^{-1}) + **1** (40 μmol L^{-1}); lane 6, DNA + mercaptoethanol (25 μmol L^{-1}); lane 7, DNA + mercaptoethanol (25 μmol L^{-1}) + **1** (40 μmol L^{-1}); lane 8, DNA + sodium ascorbate (25 μmol L^{-1})/H_2O_2 (25 μmol L^{-1}); lane 9, DNA + sodium ascorbate (25 μmol L^{-1})/H_2O_2 (25 μmol L^{-1}) + **1** (40 μmol L^{-1}); lane 10, DNA + sodium ascorbate (12.5 μmol L^{-1})/H_2O_2 (25 μmol L^{-1}); lane 11, DNA + sodium ascorbate (12.5 μmol L^{-1})/H_2O_2 (25 μmol L^{-1}) + **1** (40 μmol L^{-1}). (b) For **2**: Lane 0, DNA control; lane 1, DNA + **2** (44 μmol L^{-1}); lane 2, DNA + H_2O_2 (25 μmol L^{-1}); lane 3, DNA + H_2O_2 (25 μmol L^{-1}) + **2**(44 μmol L^{-1}); lane 4, DNA + sodium ascorbate (25 μmol L^{-1}); lane 5, DNA + sodium ascorbate (25 μmol L^{-1}) + **2** (44 μmol L^{-1}); lane 6, DNA + mercaptoethanol (25 μmol L^{-1}); lane 7, DNA + mercaptoethanol (25 μmol L^{-1}) + **2** (44 μmol L^{-1}); lane 8, DNA + sodium ascorbate (25 μmol L^{-1})/H_2O_2 (25 μmol L^{-1}); lane 9, DNA + sodium ascorbate (25 μmol L^{-1})/H_2O_2 (25 μmol L^{-1}) + **2** (44 μmol L^{-1}); lane 10, DNA + sodium ascorbate (12.5 μmol L^{-1})/H_2O_2 (25 μmol L^{-1}); lane 11, DNA + sodium ascorbate (12.5 μmol L^{-1})/H_2O_2 (25 μmol L^{-1}) + **2** (44 μmol L^{-1}).

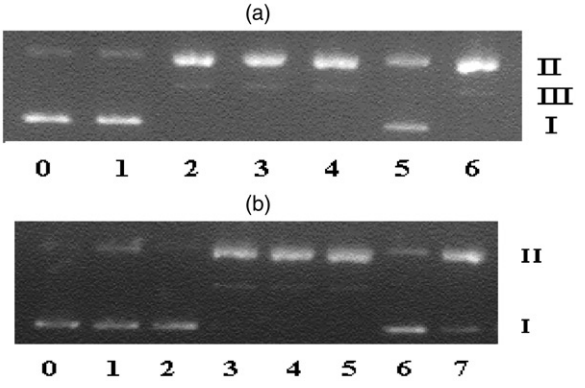

Figure 9. Agarose gel electrophoresis diagrams showing the cleavage of pBR322 DNA (33 μmol L^{-1}) by **1** or **2** treated with sodium ascorbate and potential inhibitors in Tris–HCl/NaCl buffer (50 m mol L^{-1}, pH 7.2). Incubation time: 3 h (37°C). (a) For **1**: Lane 0, DNA control; lane 1, DNA + sodium ascorbate (25 μmol L^{-1}); lane 2, DNA + **1** (80 μmol L^{-1}) + sodium ascorbate (25 μmol L^{-1}); lanes 3–6, DNA + **1** (80 μmol L^{-1}) + sodium ascorbate (25 μmol L^{-1}) + [DMSO (60 μmol L^{-1}); SOD (60 μmol L^{-1}); Histidine (60 μmol L^{-1}); MEDTA (60 μmol L^{-1}), respectively. (b) For **2**: Lane 0, DNA control; lane 1, DNA + **2** (44 μmol L^{-1}); lane 2, DNA + sodium ascorbate (25 μmol L^{-1}); lane 3, DNA + **2** (44 μmol L^{-1}) + sodium ascorbate (25 μmol L^{-1}); lanes 4–7, DNA + **2** (44 μmol L^{-1}) + sodium ascorbate (25 μmol L^{-1}) + [DMSO (60 μmol L^{-1}); SOD (60 μmol L^{-1}); Histidine (60 μmol L^{-1}); MEDTA (60 μmol L^{-1}), respectively].

partial intercalative mode. The agarose gel electrophoresis studies show that both promote the oxidative cleavage of plasmid DNA at physiological pH and temperature in the presence of reducing agents. Our investigation of the DNA cleavage mechanism suggests that singlet oxygen is the ROS that leads to DNA cleavage.

Supplementary material

Crystallographic data of **1** and **2** (excluding structure factors) for the structural analysis have been deposited with the Cambridge Crystallographic Data Centre with CCDC No. 668143 (**1**), 657338 (**2**). Copies of this information may be obtained free of charge from the Director, CCDC, 12 Union Road, Cambridge, CB2 1EZ, UK (Fax: +44 1223 336 033; E-mail: deposit@ccdc.cam.ac.uk or www: http://www.ccdc.cam.ac.uk).

Acknowledgments

This study was supported by the National Natural Science Foundation of China (No. 21001066) and the Fundamental Research Funds for the Central Universities.

References

[1] P.U. Maheswari, S. Roy, H. Dulk, S. Barends, G. Wezel, B. Kozlevcar, P. Gamez, J. Reedijk. *J. Am. Chem. Soc.*, **128**, 710 (2006).
[2] P.U. Maheswari, K. Lapplainen, M. Sfregola, S. Barends, P. Gamez, U. Turpeinen, I. Mutikainen, G. Weze, J. Reedijk. *Dalton Trans.*, 3676 (2007).

[3] J. Qian, W. Gu, H. Liu, F.X. Gao, L. Feng, S.P. Yan, D.Z. Liao, P. Cheng. *Dalton Trans.*, 1060 (2007).
[4] M. Roy, B. Pathak, A.K. Patra, E.D. Jemmis, M. Nethaji, A.R. Chakravarty. *Inorg. Chem.*, **46**, 11122 (2007).
[5] Y. An, M.L. Tong, L.N. Ji, Z.W. Mao. *Dalton Trans.*, 2066 (2006).
[6] J.L. Tian, L. Feng, W. Gu, G.J. Xu, S.P. Yan, D.Z. Liao, Z.H. Jiang, P. Cheng. *J. Inorg. Biochem.*, **101**, 196 (2007).
[7] C.A. Mitsopoulou, C.E. Dagas, C. Makedonas. *J. Inorg. Biochem.*, **102**, 77 (2008).
[8] H. Sigel, A. Sigel. *Interactions of Metal Ions with Nucleotides, Nucleic Acids, and Their Constituents*, Dekker, New York (1996).
[9] B.C.G. Soderberg. *Coord. Chem. Rev.*, **252**, 57 (2008).
[10] N. Farrell. *Transition Metals as Drugs and Chemotherapeutic Agents*, Springer, The Netherlands (1989).
[11] T.D. Tullius, J.A. Greenbaum. *Curr. Opin. Chem. Biol.*, **9**, 127 (2005).
[12] G.F. D'Alelio, E.T. Hofman, J.R. Zeman. *J. Macromol. Sci., Part A: Pure Appl. Chem.*, **3**, 959 (1969).
[13] K. Tatsumoto, A.E. Martell. *J. Am. Chem. Soc.*, **103**, 6203 (1981).
[14] K. Tatsumoto, A.E. Martell, R.J. Motekaitis. *J. Am. Chem. Soc.*, **103**, 6197 (1981).
[15] H.M. Dawes, J.M. Waters, T.N. Waters. *Inorg. Chim. Acta*, **66**, 29 (1982).
[16] I. Bkouche-Waksman, J.M. Barbe, A. Kvick. *Acta Crystallogr., Sect. B*, **44**, 595 (1988).
[17] R. Hamalainen, U. Turpeinen. *Acta Crystallogr., Sect. C*, **41**, 1726 (1985).
[18] K. Korhonen, R. Hamalainen, U. Turpeinen. *Acta Crystallogr., Sect. C*, **40**, 1175 (1984).
[19] K. Nakagima, M. Kojima, K. Foriumi, K. Saito, J. Fujita. *Bull. Chem. Soc. Jpn.*, **62**, 760 (1989).
[20] V. Kettmann, E. Fresova. *Acta Crystallogr., Sect. C*, **49**, 1932 (1993).
[21] C.T. Yang, B. Moubaraki, K.S. Murray, J.J. Vittal. *J. Chem. Soc., Dalton Trans.*, **5**, 880 (2003).
[22] C.T. Yang, M. Vetrichelvan, X. Yang, B. Moubaraki, K.S. Murray, J.J. Vittal. *J. Chem. Soc., Dalton Trans.*, **1**, 113 (2004).
[23] M.A. Alam, M. Nethaji, M. Ray. *Angew. Chem., Int. Ed.*, **42**, 1940 (2003).
[24] J.D. Ranford, J.J. Vittal, D. Wu. *Angew. Chem., Int. Ed.*, **37**, 1114 (1998).
[25] J.D. Ranford, J.J. Vittal, D. Wu, X. Yang. *Angew. Chem., Int. Ed.*, **38**, 3498 (1999).
[26] X. Yang, J.D. Ranford, J.J. Vittal. *Cryst. Growth Des.*, **4**, 781 (2004).
[27] X. Yang, D. Wu, J.D. Ranford, J.J. Vittal. *Cryst. Growth Des.*, **5**, 41 (2005).
[28] C.T. Yang, B. Moubarki, K.S. Murray, J.D. Ranford, J.J. Vittal. *Inorg. Chem.*, **40**, 5934 (2001).
[29] C.T. Yang, J.J. Vittal. *Inorg. Chim. Acta*, **344**, 65 (2003).
[30] B. Sreenivasulu, M. Vetichelvan, F. Zhao, S. Gao, J.J. Vittal. *Eur. J. Inorg. Chem.*, **22**, 4635 (2005).
[31] B. Sreenivasulu, J.J. Vittal. *Cryst. Growth Des.*, **3**, 635 (2003).
[32] K.E. Voss, R.J. Angelici, R.A. Jacobson. *Inorg. Chem.*, **17**, 1922 (1978).
[33] X.F. Ma, J.L. Tian, W. Gu, S. Gao, S.P. Yan, D.Z. Liao. *Inorg. Chem. Commun.*, **11**, 256 (2008).
[34] (a) K.W. So, C.T. Yang, J.J. Vittal, J.D. Ranford. *Inorg. Chim. Acta*, **349**, 135 (2003); (b) X. Wang, J. Ding, J.J. Vittal. *Inorg. Chim. Acta*, **359**, 3481 (2006).
[35] M.A. Alam, R.R. Koner, A. Das, M. Nethaji, M. Ray. *Cryst. Growth Des.*, **7**, 1818 (2007).
[36] M.A. Alam, M. Nethaji, M. Ray. *Angew. Chem. Int. Ed. Engl.*, **42**, 1940 (2003).
[37] G.M. Sheldrick, *SADABS 2.05*, University of Gottingen, Germany (2002).
[38] *SHELXTL 6.10*. Bruker Analytical Instrumentation, Madison, WI, USA (2000).
[39] J. Marmur. *J. Mol. Biol.*, **3**, 208 (1961).
[40] M.E. Reichmann, S.A. Rice, C.A. Thomas, P. Doty. *J. Am. Chem. Soc.*, **76**, 3047 (1954).
[41] A. Wolfe, G.H. Shimer Jr, T. Meehan. *Biochemistry*, **26**, 6392 (1987).
[42] J. Bermadou, G. Pratviel, F. Bennis, M. Girardet, B. Meunier. *Biochemistry*, **28**, 7268 (1989).
[43] F.V. Pamatong, C.A. Detmer, J.R. Bocarsly. *J. Am. Chem. Soc.*, **118**, 5339 (1996).
[44] J.K. Barton, A.T. Danishefsky, J.M. Goldberg. *J. Am. Chem. Soc.*, **106**, 2172 (1984).
[45] J.M. Kelly, A.B. Tossi, D.J. McConnel, C. Ohuigin. *Nucleic Acids Res.*, **13**, 6017 (1985).
[46] S.A. Tysoe, A.D. Baker, T.C. Strekees. *J. Phys. Chem.*, **97**, 1707 (1993).
[47] K.G. Strothkamp, R.E. Strothkamp. *J. Chem. Educ.*, **71**, 77 (1994).
[48] J.B. Lepecq, C. Paoletti. *J. Mol. Biol.*, **27**, 87 (1967).
[49] N. Raman, A. Sakthivel, R. Jeyamurugan. *J. Coord. Chem.*, **63**, 1080 (2010).